Available online at www.sciencedirect.com
SCIENCE DIRECT
Biochemical and Biophysical Research Communications 347 (2006) 301–309
BBRC
www.elsevier.com/locate/ybbrc

# Identification of an intermolecular disulfide bond in barley hemoglobin ☆

Natalia V. Bykova [b,1], Abir U. Igamberdiev [a], Werner Ens [b], Robert D. Hill [a,*]

[a] Department of Plant Science, University of Manitoba, Winnipeg, Man., Canada R3T 2N2
[b] Department of Physics and Astronomy, University of Manitoba, Winnipeg, Man., Canada R3T 2N2

Received 7 June 2006
Available online 22 June 2006

**Abstract**

Barley class-1 hemoglobin (Hb) and its mutated version ($Cys^{79}$ replaced by Ser) were overexpressed in *Escherichia coli* and purified to near homogeneity. Nano-electrospray ionization mass spectrometry (nano-ESI MS) showed that the mutated barley Hb was more readily dissociated to a monomer and was more susceptible to denaturation than the native form. The mutated Hb was oxidized to the ferric state $\sim 10^3$ times faster than the non-mutated form. The increased oxidation of the mutated Hb was a result of substitution of the cysteine with a serine and not a consequence of monomer formation, *per se.* Tandem mass spectrometry (MS/MS) analysis revealed that $Cys^{79}$ participated in intermolecular S–S bond formation. The rates of nitric oxide scavenging by non-mutated and mutated Hb were similar. We conclude that the cysteine residue is an important contributor to the quaternary and tertiary structure of barley hemoglobin. It however has no direct effect on nitric oxide-scavenging activity of barley Hb.


*Keywords:* Barley hemoglobin; Cysteine; Dimer; Disulfide bond; Mass spectrometry; Nitric oxide

Class-1 plant hemoglobins are induced by hypoxia and participate in NO metabolism [1–4]. Most investigated class-1 hemoglobins have a single conserved cysteine residue located in the E-helix of the polypeptide chain [5]. This helix is bent toward the center of the porphyrin ring due to a direct coordination of His(E7) with the iron atom [5]. *Arabidopsis* class-1 hemoglobin has two cysteine residues per monomer [6] located adjacent one to another in the same position where a single cysteine is found in other class-1 hemoglobins.

Other groups of hemoglobins may vary in the abundance of cysteine residues. Most plant leghemoglobins do not contain cysteines at all [7,8]. Human blood hemoglobin contains two cysteine residues in the β-chain and one in the α-chain. Cysteine-93 of the β-chain contributes to the maintenance of cooperativity and ligand binding [9]. Human myoglobin contains a single cysteine having a role in reduction of heme iron, a process during which the intermolecular disulfide bond is likely formed [10]. Human neuroglobin, which resembles plant class-1 hemoglobin in hexacoordination of heme and high affinity for $O_2$ and NO, contains three cysteine residues, which participate in formation of intra- and intermolecular disulfide bonds depending on the redox state of the environment [11]. Two intermolecular disulfide bonds involving $Cys^{38}$ and $Cys^{83}$ support the dimeric structure of another human hexacoordinate hemoglobin, cytoglobin [12]. Both inter- and intramolecular disulfide bond formation has been demonstrated in other hemoglobins [13–16].

Barley hemoglobin, the class-1 plant hemoglobin, was found to be a homodimer [17] containing a single cysteine ($Cys^{79}$) per monomer unit [1,17]. The existing model of the tertiary structure of the class-1 rice Hb, which has very

☆ *Abbreviations:* Hb, hemoglobin; rHb, recombinant non-mutated barley Hb; mutHb, recombinant barley Hb with replacement of $Cys^{79}$ by Ser; MS, mass spectrometry; MS/MS, tandem mass spectrometry; MALDI Qq-TOF, matrix-assisted laser desorption/ionization quadrupole–quadrupole-time-of-flight; TCEP, tris(2-carboxyethyl)phosphine.

* Corresponding author. Fax: +1 204 474 7528.
*E-mail address:* rob_hill@umanitoba.ca (R.D. Hill).
[1] Present address: Agriculture and Agri-Food Canada, Cereal Research Centre, Winnipeg, Man., Canada R3T 2M9.

0006-291X/$ - see front matter © 2006 Elsevier Inc. All rights reserved.
doi:10.1016/j.bbrc.2006.06.091

similar structure to the barley Hb, does not involve S–S bond formation between subunits [5]. According to this model, the monomeric units are associated via coordination bonds on the surface and do not involve the cysteine residue. This interaction is however quite weak ($K_d$ 86 μM) and cannot explain the prevalence of the dimeric form even in diluted solutions.

To investigate the contribution of the cysteine to the physico-chemical characteristics of the barley Hb molecule, we prepared a recombinant, mutated barley Hb in which the unique cysteine ($Cys^{79}$) residue is replaced by serine. Our data indicate that the mutation affects the structural stability of the molecule and increases its susceptibility to auto-oxidation. Mass spectrometry analysis revealed that Cys directly participates in S–S bond formation between subunits.

## Materials and methods

*Mutation of barley recombinant hemoglobin, its purification and peptide mass mapping.* Site-directed mutagenesis of $Cys^{79}$ (TGC) to $Ser^{79}$ (AGC) in barley hemoglobin was performed using the QuikChange Site-Directed Mutagenesis Kit (Stratagene). A forward primer consisting of 5′-CC GTG TCC GTC TTC GTC ATG ACC AGC GAG GCG GC-3′ with the reverse primer being 5′-GC CGC CTC GCT GGT CAT GAC GAA GAC GGA CAC GG-3′ were used. The underlined sequence indicates the triplet coding for the altered amino acid. Preparation of extracts and purification of recombinant hemoglobin from *Escherichia coli* strain DH-5α (Invitrogen, Canada) was conducted as described previously [4]. Purified hemoglobin fractions had a ratio of absorbance at 412 nm to absorbance at 280 nm in the range 3.0–3.2, corresponding to 90–95% purity. Peptide mass mapping and tandem mass spectrometry analyses of tryptic peptides were performed as described earlier [4] using digestion with modified trypsin [18] and purification of the tryptic peptide mixture on a reverse-phase POROS R2 (20–30 μm bead size, PerSeptive Biosystems, Framingham, CA, USA) nanocolumn [19]. MS and MS/MS analyses were performed by MALDI Qq-TOF mass spectrometer (Manitoba/Sciex prototype) [20,21].

*Electrospray ionization mass spectrometry analysis of intact proteins (ESI-MS).* ESI-MS analysis was performed using a hybrid quadrupole time-of-flight mass spectrometer API QSTAR Pulsar *i* (AB-MDS Sciex, Toronto, Canada) equipped with a nano-electrospray source (Protana Engineering, Odense, Denmark). The nano-ESI-MS system was mass calibrated with a mixture of CsI and sex pheromone inhibitor iPD1 in 50% methanol, 2% acetic acid. Samples were exchanged into 20 mM ammonium bicarbonate buffer, diluted to a final concentration of 10 μM protein, and loaded directly into pre-coated borosilicate nano-electrospray needles (Protana Engineering, Odense, Denmark). An ion spray voltage of 1.1 kV, ion source temperature of 20 °C, and de-clustering potential of 80 V between the orifice and skimmer were set to preserve the heme–protein complex and afford charge-state distributions largely for the holo-Hb form of the protein. The de-convolution mass analysis was performed using BioAnalyst extensions available in Analyst QS software (AB-MDS Sciex, Toronto, Canada). For determination of the intact protein mass under denaturing conditions, protein solutions were 1:1 diluted in acetonitrile containing 2% acetic acid. Mass determinations were performed for at least two independent protein preparations. Mass values refer to means ± SD from $\geqslant 5$ analyses.

*Determination of disulfide bond formation by MALDI-MS and MS/MS.* Purified rHb and mutant protein were dialyzed against 100 mM $NH_4HCO_3$ and directly digested with trypsin. The resulting tryptic fragments were analyzed by MALDI mass spectrometry and peptide mass mapping in order to identify a candidate fragment containing a disulfide bond. The candidate disulfide bond-containing ion fragment was further subjected to low-energy collision-induced dissociation and tandem mass spectrometry analysis. Proteins were also reduced with 10 mM DTT at 56 °C for 30 min and alkylated at room temperature with 55 mM iodoacetamide prior to digestion and peptide mass mapping analysis. A differential alkylation experiment was carried out where protein was first treated with 55 mM iodoacetamide, extensively dialyzed against 100 mM $NH_4HCO_3$, completely reduced with 10 mM DTT at 56 °C, and then alkylated with 55 mM iodoacetic acid.

*Auto-oxidation of barley hemoglobin.* Auto-oxidation of 20 μM rHb and mutHb was determined by following absorbance at 576 nm in 50 mM Tris–HCl buffer, pH 8.0. Extinction coefficients of 17.3 and 9.2 $mM^{-1}\,cm^{-1}$ were used for the reduced, ferrous oxy form and oxidized ferric form of Hb [17]. The data were fitted to a single-exponential decay expression. Reduction of the disulfide bond was accomplished by treating rHb with either 1 mM TCEP for 2 h at room temperature or 10 mM DTT for 1 h at 45 °C. The excess of reducing reagent was removed via a P-2 column (0.5 × 2 cm) (Bio-Rad, Canada).

## Results

### *Identification of rHb and mutHb*

The mutation in barley Hb was identified by DNA sequencing and MS/MS analysis. DNA sequencing revealed the replacement of TGC to AGC, i.e., only one nucleotide (T in position 297 replaced by A). The mass of the protein monomer assessed from the intact protein nano-ESI MS was determined as 18,625 ± 2 Da. Translation of the recombinant protein sequence as presented in [17] leads to a protein mass of 18,538, excluding the mass of covalently bound heme. The average molecular weight of the mutant barley Hb monomer was 18,641 ± 3 Da. The measured mass difference of 16 Da between the recombinant and mutant barley Hb is in agreement with the mass difference between cysteine and serine residues. Analysis of tryptic digests by matrix-assisted laser desorption ionization-time-of-flight confirmed substitution of the cysteine residue in the recombinant barley Hb to serine in the mutant Hb (Fig. 1).

Size-exclusion chromatography, at two different rHb concentrations, indicated a major peak with a molecular mass of ~40 kDa, corresponding to a dimer (Fig. 2A and D), with small amounts (<5%) of a monomeric peak (~19 kDa). Reduction with TCEP resulted in a substantial increase in the monomeric peak, with the dimeric peak being a minor component at the lower rHb concentration (Fig. 2B and E). Chromatography of the mutHb gave prominent peaks corresponding to a monomer and dimer (Fig. 2C and F), with the monomer comprising ~30% of the total mutHb when the concentrated mutHb was loaded on the column increasing to ~50% when the protein concentration was decreased by one half.

### *Mass spectrometry characterization of the recombinant and mutant barley Hb*

In Fig. 3A, the nano-electrospray ionization mass spectrum of rHb, sprayed at a protein concentration of 10 μM under pseudo-physiological conditions from aqueous

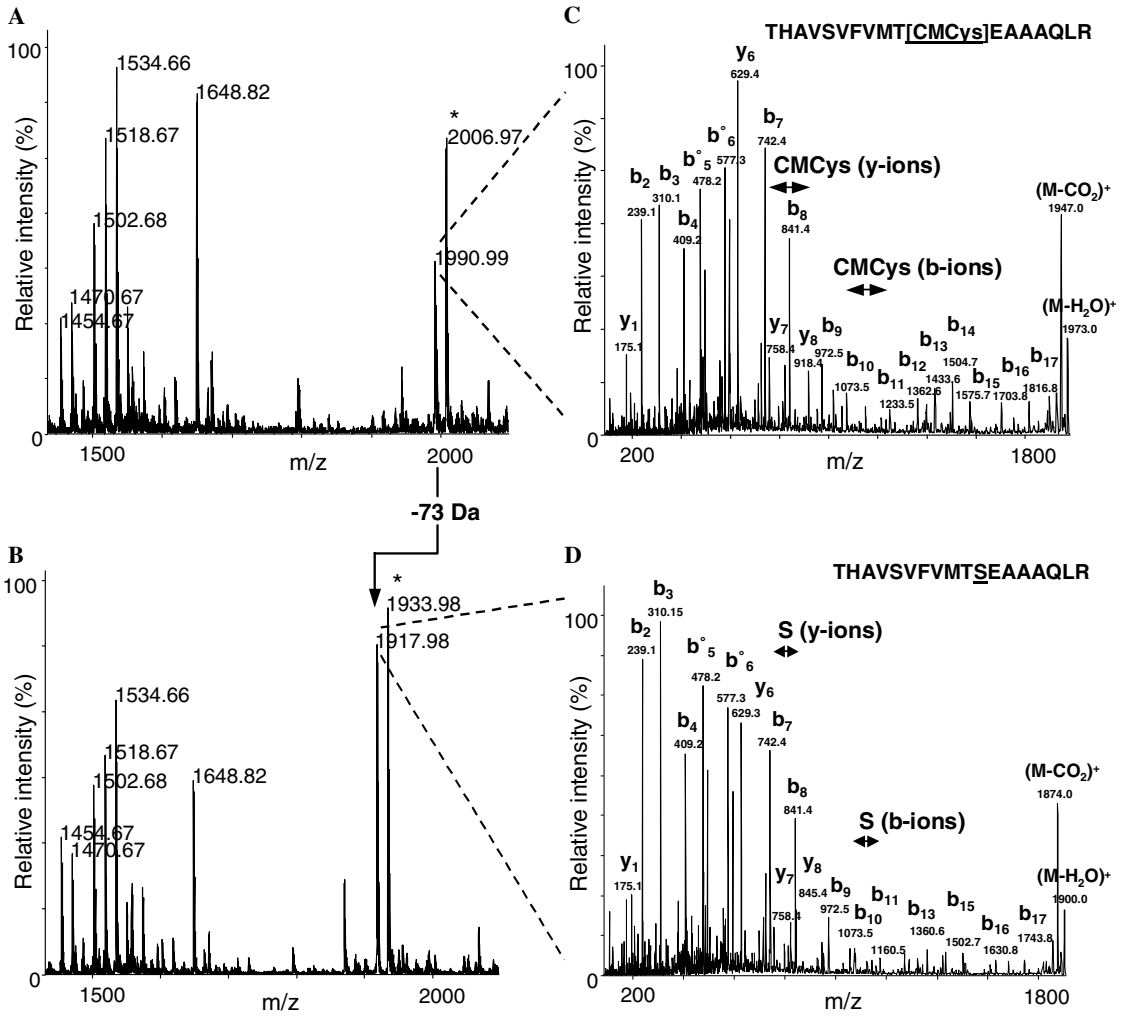


Fig. 1. The site of mutagenesis in recombinant barley Hb. (A,B) MALDI Qq-TOF MS peptide mass mapping analysis of peptide mixtures generated by in situ digested SDS–PAGE bands of the purified rHb and mutHb, respectively. Note that cysteine residue was derivatized to *S*-carbamidomethyl-cysteine during sample preparation. The arrow indicates difference in 73 Da between the rHb peptide mass (peptide ion at *m*/*z* 1990.99 in (A)) and mutHb peptide mass (peptide ion at *m*/*z* 1917.98 in (B)). Due to partial oxidation of methionine (+16 Da), peptides of interest ion signals were accompanied by the satellite ion signals (indicated with asterisk). Tandem MS spectra obtained using collision-induced dissociation (CID) of the corresponding precursor peptide (C,D) and performed directly after peptide mass mapping exhibited a number of sequence-specific peptide fragment b- and y-ion signals. The mass difference of 160 Da between y8 and y7 ions as well as between b11 and b10 ions assigned the presence of carbamidomethyl-cysteine (CMCys) in rHb peptide (C), which was substituted to serine in mutant peptide with mass difference 87 Da between the identical ions (D). The peaks denoted b° are the result of water (−18 Da) losses from corresponding ion.

20 mM ammonium bicarbonate-buffered at pH 8.0 solutions, is shown. The detection of large non-covalent assemblies (exhibiting higher *m*/*z* values) was enhanced by optimizing electrospray conditions (as described in Materials and methods). Ions from the dimer were the most abundant and the ion envelope of the folded monomer also started to appear in the spectrum due to subunit dissociation. The stable form of the protein also has one heme per subunit. De-convolution of these data gives one major peak at an average mass of 38,717 Da corresponding to a dimer holoprotein and a smaller peak at an average mass of 19,359 Da corresponding to a monomer holoprotein (Fig. 3C).

The nano-electrospray ionization mass spectrum of the mutant barley Hb, sprayed under exactly the same experimental conditions and protein concentration of 10 μM, was more complex (Fig. 3B). Three distinct charge envelopes, representing ions from an unfolded monomer, a folded monomer, and a dimer, could be seen. However, only very small ion signals originating from dimeric species were observed (less than 10% of the total ion current). The apoprotein form also started to appear with a concomitant increase of a singly charged ion at *m*/*z* 616 corresponding to a heme. The de-convolution shows clearly that the monomer holoprotein was dominating in the spectrum (Fig. 3D). The protein with a substituted cysteine residue is more easily denatured.

It should be noted that in both the rHb and mutHb, the $M_r$ detected corresponds to the $[M + nNH_3]^+$ ion commonly seen in the presence of $NH_4^+$ salt spraying

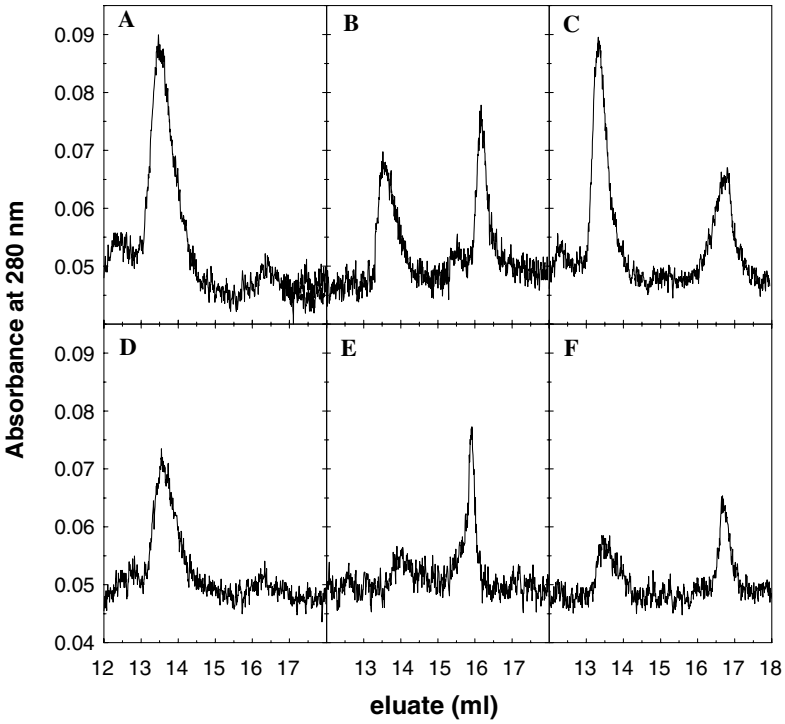


Fig. 2. Elution profiles of recombinant non-mutated (A, B, D, and E) and mutated (C,F) barley hemoglobins from a Superose 12 column. Concentration of Hb loaded on the column was 24 μM (A–C) and 12 μM (D–F). (B,E) Reduced with TCEP.

conditions. For the rHb protein it corresponds to a 12 $NH_3$ mass increase of the folded monomer and 24 $NH_3$ mass increase of the dimer. The mass increase of the mutant monomer corresponded to 6 $NH_3$, and of the dimer, 17 $NH_3$.

Addition of cofactors NADH and FAD (also desalted into ammonium bicarbonate buffer) at two different concentrations 3 and 30 μM did not change the protein spectra of either rHb or mutHb under native conditions indicating the absence of non-covalent interaction between Hb and these cofactors.

*Identification of a disulfide bridge between cysteine residues by mass spectrometry*

To check whether the intermolecular disulfide bond formation as a posttranslational event is associated with three-dimensional folding of the plant Hb homodimeric structure, MALDI peptide mass mapping analysis comparing non-reduced and reduced plus alkylated digests of rHb and mutHb protein was performed. The spectrum in Fig. 4A demonstrates a tryptic fragment ion with *m*/*z* 3864.98 which was observed in digests of non-reduced rHb. This fragment was not present, neither in reduced and alkylated rHb nor in mutHb protein digests. However, a new ion with *m*/*z* 1990.99 was detected in a spectrum of reduced and alkylated rHb digest (Fig. 4B). The peptide with mass 3864.98 was a candidate for a disulfide bond-containing fragment ion and it corresponded to the protonated sum of two identical trypsin-derived Hb sequences THAVSVFVMTCEAAAQLR with non-reduced cysteine residues. The peptide with mass 1990.99 corresponded to the mass of the same protonated single sequence fragment but with a carbamidomethylated cysteine residue, resulting in a mass increase of 57 Da. The position of carbamidomethylated cysteine was assigned by fragmentation of this peptide in MS/MS experiment.

The differential alkylation-labeling experiment was conducted where protein was treated with iodoacetamide (+57 Da) prior to digestion in order to alkylate any cysteine residues with free –SH groups present in the solution due to the partial reduction and dissociation of Hb homodimer. The excess iodoacetamide was removed, and then the protein was fully reduced and alkylated with iodoacetic acid (+58 Da). The fragments carboxymethylated with iodoacetic acid displayed a mass shift 1 Da greater than those alkylated with iodoacetamide (peaks at *m*/*z* 1990.99 and 1991.99 in Fig. 4C). The relative intensities of the peaks corresponding to iodoacetamide/iodoacetic acid alkylated peptides provided semi-quantitative information about the degree of Cys reduction and indicated that the major portion of the Cys was involved in –S–S– bond formation.

The candidate disulfide bond-containing peptide was further subjected to direct MALDI MS/MS analysis with low-energy CID. The MS/MS spectrum of the isolated parent ion at *m*/*z* 3864.98 (Fig. 4D) displayed a characteristic triplet of intense dominating fragment ions at *m*/*z* 1899.9, 1931.9–1933.9, and 1965.9. This type of fragmentation pattern was previously described for

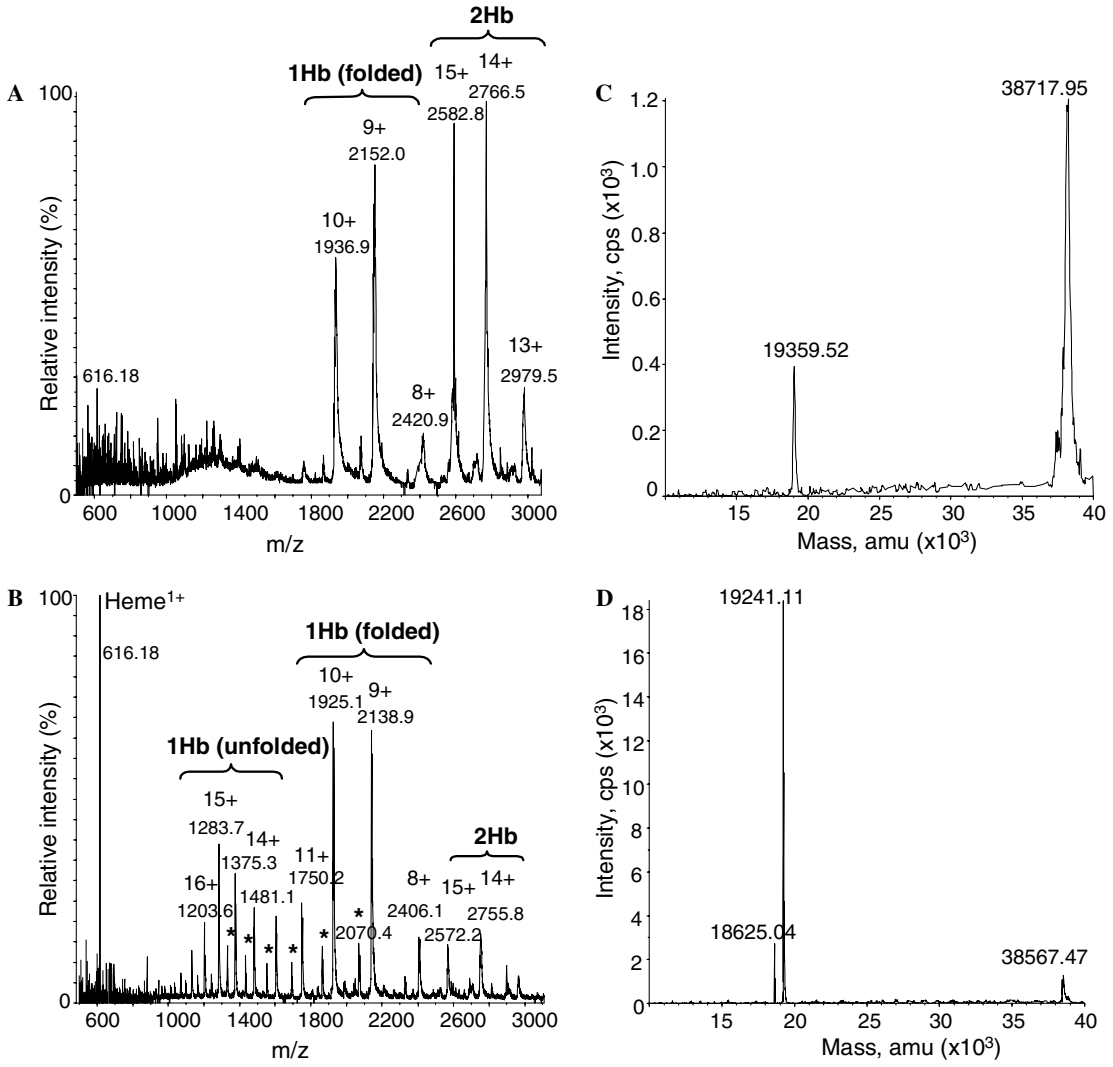


Fig. 3. Mass spectrometric analysis of the native intact recombinant and mutant barley Hb. Solutions of recombinant non-mutated (A) and mutant (B) barley holo-Hb (10 μM protein sprayed in 20 mM $NH_4HCO_3$ at pH 8.0) were analyzed by nano-ESI-MS. All experimental conditions were identical. The positive charge states are numerically labeled; monomeric form (1Hb); dimeric form (2Hb); apo-form (*). (C,D) The de-convoluted mass values for corresponding *m/z* distributions for rHb and mutHb, respectively. The data represent five analyses using two different Hb preparations. amu, atomic mass units.

spectra of interchain disulfide-linked peptides in both the collisionally induced dissociation [22] and postsource decay [23] modes. The characteristic triplet with a mass separation of 32–34 Da generated by both symmetric and non-symmetric cleavages of the disulfide bond [24] corresponds to the retention of zero, one, or two sulfurs on the charged fragments. Non-symmetric cleavage with retention of the sulfurs was found to be enthalpically favored over symmetric fragmentation or complete release of sulfurs [22]. The daughter ions carrying the intact –S–S– bridge were also observed in the spectrum as indicated in the right part of the Fig. 4D. In addition, the b and y fragment ion series specific for the sequence were present in the lower *m/z* range (Fig. 4D). These results allowed for the unambiguous identification of a disulfide bridge between two monomeric subunits of rHb dimer protein.

*Spectral properties of recombinant and mutated barley Hb*

Purified rHb had an absorbance spectrum characteristic of the ferrous oxyHb form (Fig. 5A) with prominent maxima at 540 and 576 nm [17]. It retained the ferrous oxyHb form after weeks of storage at −80 °C and slowly turned to ferric metHb at +4 °C, characterized by a maximum at 534 nm with a small shoulder at 565 nm [17]. Addition of 0.1 mM NADH or NADPH (in the presence of 5 μM FAD) at 25 °C resulted in slow reversion of the ferric metHb form to the oxyHb form at a rate of 6–7 nmol $min^{-1}$ $mg^{-1}$ protein (Fig. 5). Purified mutHb showed a different spectrum, with a smaller right shoulder (Fig. 5B), corresponding to a mixture of the ferrous oxyHb and ferric metHb forms.

The addition of sodium dithionite resulted in appearance of the same deoxy form in both rHb and mutHb. Removal of dithionite on a P-2 column resulted in appearance of the oxy

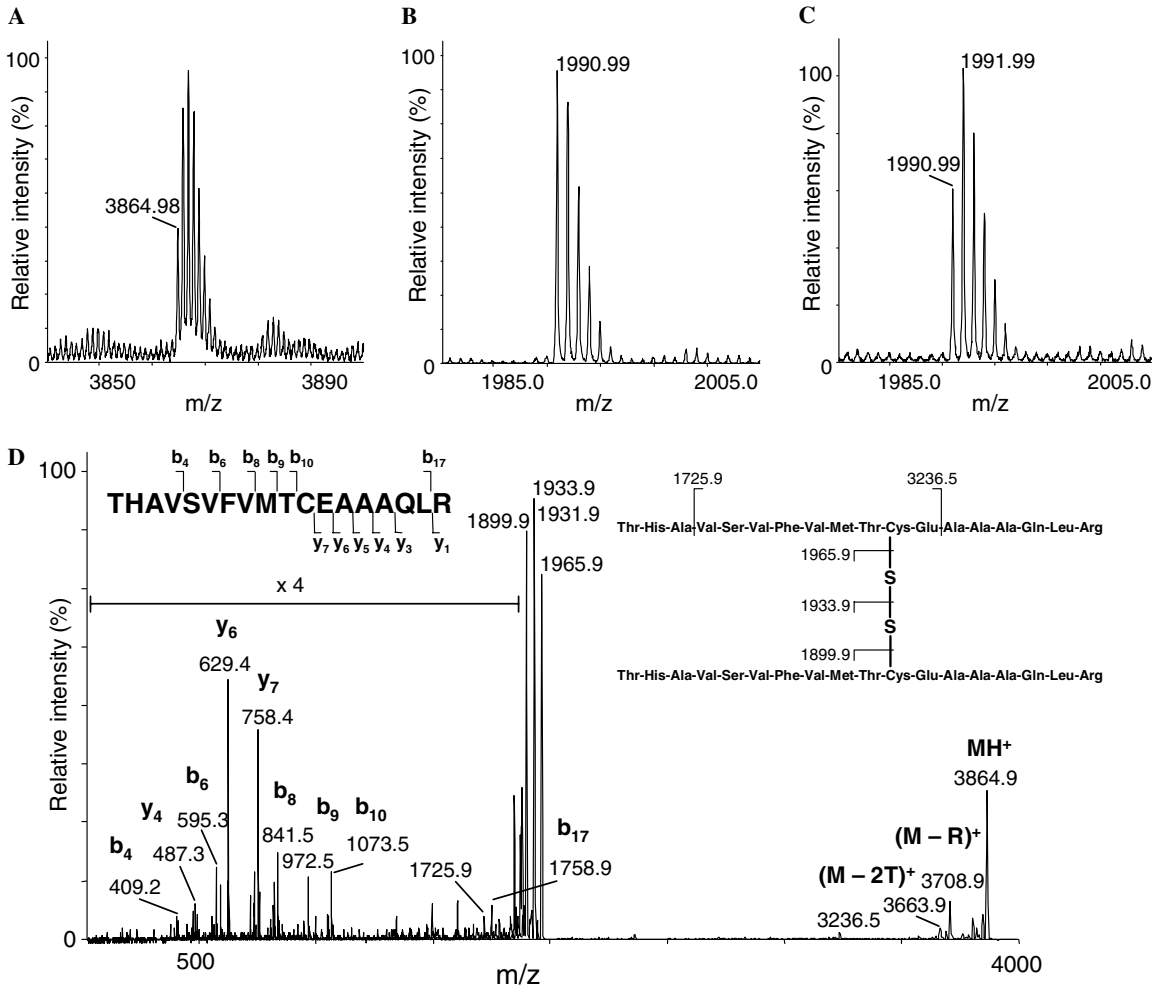


Fig. 4. MALDI-MS and MS/MS identification of the disulfide bond in recombinant barley hemoglobin. (A) Candidate disulfide bond-containing tryptic fragment ion present in protein digest under non-reducing conditions. (B) Tryptic fragment ion appeared after complete reduction and alkylation with iodoacetamide. (C) The peaks with 1 Da mass difference appeared after differential iodoacetamide/iodoacetic acid treatment. (D) MS/MS spectra of the tryptic peptide parent ion at *m*/*z* 3864.98, carrying an interchain disulfide bond. The dominating daughter ions at *m*/*z* 1899.9–1931.9 and 1933.9–1965.9 correspond to the –S–S– bridge cleavage. The sequence-specific peptide fragment b- and y-ion signals are indicated on the left side of panel and the ions carrying the intact –S–S– bridge are schematically represented on the right side of panel. The detection of ion at *m*/*z* 3708.9 indicated the loss of an Arg residue from the parent ion following cleavage of the amide bond from either peptide, while the loss of Thr residues from both peptides resulted in the ion at *m*/*z* 3663.9.

form similar to that of rHb, which rapidly turned to the ferric form in the case of the mutHb. The auto-oxidation rate of mutHb was about three orders of magnitude faster than that of rHb, with a half-life for the ferrous oxy form of ~72 h for rHb compared to ~0.1 h for mutHb (Fig. 6).

The reduction of the disulfide bond in rHb by TCEP did not significantly increase the rate of rHb auto-oxidation (Fig. 6A, line 2). There was no effect of TCEP on the rate of auto-oxidation of the mutated Hb. The reduction of Hb by DTT (not shown) resulted in exactly the same rate of auto-oxidation as the reduction by TCEP.

*NO-scavenging activity of recombinant and mutated Hb*

The purified rHb and mutHb possessed low, sustained NO-scavenging activities in the presence of NADH or NADPH. The activity was not inhibited by pHMB (Table 1). The activity measured spectrophotometrically at 340 nm by oxidation of NADH or NADPH with NO supplied by DEANO stoichiometrically corresponded to the NO decline, representing one mole of NAD(P)H consumed per two moles of NO (Table 1). The activity with NADH was slightly higher than with NADPH; however, the precision of measurements at such low rates does not allow definitive conclusion on the preference of NADH over NADPH.

## Discussion

Roles of cysteine in enzyme molecules include participation in catalysis and formation of intramolecular and intermolecular disulfide bonds. There are also some cases when cysteines are not essential, neither for catalysis nor for disulfide bond formation, but participate in stabilization

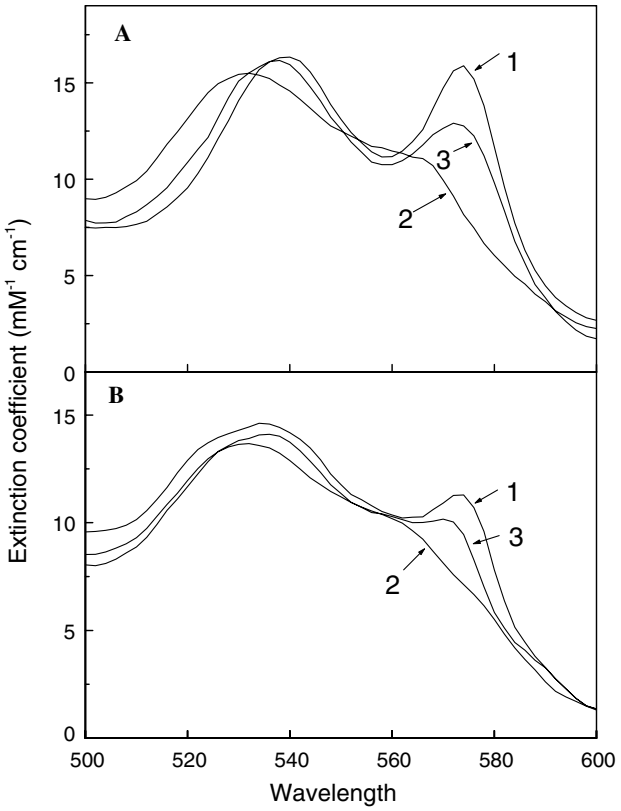


Fig. 5. Absorbance spectra (A,B) recorded between 500 and 600 nm of recombinant (A) and mutated (B) barley Hb. 1, Immediately after purification; 2, after oxidation to ferric form; 3, after partial reduction by NADH.

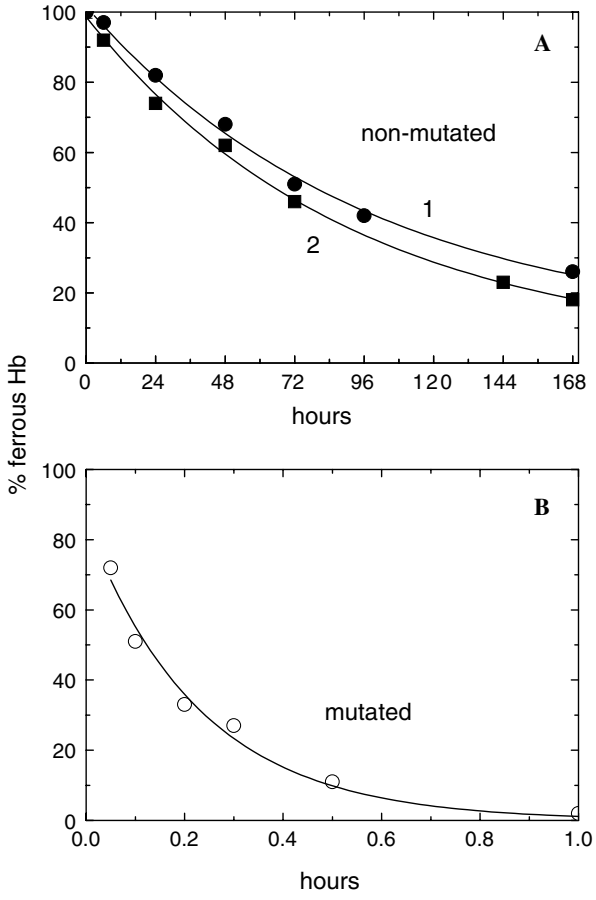


Fig. 6. Time course of the auto-oxidation of recombinant (A) and mutated (B) barley Hb. The percent of the ferrous form was determined from the optical density at 576 nm. 1, Auto-oxidation of untreated Hb; 2, Hb auto-oxidation after the reduction of the S–S bond with TCEP.

of the quaternary or tertiary structure and substrate/cofactor binding [25]. In globins, cysteine residues occur at well-defined positions, suggesting specific functions. In neuroglobin and cytoglobin, cysteines participate in formation of intramolecular disulfide bonds in response to the redox state of the cell [12], while intermolecular disulfide bonds in neuroglobin [11] and cytoglobin [26] were also demonstrated. The intramolecular disulfide bridge formation causes structural changes of the heme pocket, which is more expressed in neuroglobin than in cytoglobin [12,27]. Barley Hb has only one cysteine per monomer so an intramolecular disulfide bond is excluded, while adjacent cysteine residues in *Arabidopsis* class-1 Hb [6] may form a link depending on the redox state of the molecule. In human myoglobin, the cysteine residue may participate directly in reduction of heme iron, which results in intermolecular disulfide bond formation [10]. This bond is not permanent and appears as a part of the reduction–oxidation cycle of myoglobin molecule.

Disulfide bond formation in barley Hb would require interaction of the E helix of each subunit [5]. However, the S–S bond is likely to be not the only factor for dimer formation as a portion of mutHb was found to be in a dimeric form (Figs. 2 and 4). This is consistent with the proposed non-covalent interaction, occurring in the region of the G helix and in the region between the B and C helices [5]. Dimers involving disulfide bond formation would require interaction of the E helix of each subunit, which may stabilize non-covalent interaction between the monomers. The disulfide bond is hydrophobic and contributes to the folding, stability, and reactivity of the protein [10].

For neuroglobin, a hexacoordinate hemoglobin abundant in mammalian neural tissue and having similar ligand-binding properties as class-1 plant hemoglobins, it has been already shown that it is present as a mixture of monomer, dimer, and tetramer. The addition of DTT abolished the presence of aggregates, suggesting that dimerization is based on disulfide bridging [11]. In neuroglobin, the disulfide bond is involved in protein stability via modification of affinity of the iron atom for the distal histidine [28].

The amino acid substitution in mutHb resulted in easier oxidation of the heme. Conversion of mutHb to the ferric form occurs rapidly over time, with the rate being $\sim 10^3$ times faster than the oxidation of rHb (Fig. 6). $Cys^{79}$ may, therefore, play a role in maintenance of the heme in a reduced state. Slow reduction of the protein by NADH, however, demonstrates that the transition between the ferric and ferrous forms is reversible. Dimerization via an intermolecular disulfide bond is possible for the β-subunit of human Hb, when it is expressed without the α-subunit

Table 1
Rates of NO conversion and NAD(P)H oxidation (in nmol $min^{-1}$ $mg^{-1}$ Hb protein) by barley non-mutated and mutated Hb (mean values ± SD from 5 to 8 measurements)

| Hb | pHMB | NADH-dependent NO decline | NADH decline | NADPH-dependent NO decline | NADPH decline |
|---|---|---|---|---|---|
| Non-mutated | − | 13.4 ± 3.3 | 5.9 ± 0.8 | 8.1 ± 2.3 | 4.1 ± 0.9 |
| | + | 14.1 ± 2.7 | 6.1 ± 0.9 | 8.7 ± 1.8 | 4.8 ± 1.6 |
| Mutated | − | 12.7 ± 3.8 | 6.9 ± 0.2 | 9.2 ± 1.4 | 4.7 ± 0.5 |
| | + | 11.9 ± 2.8 | 6.7 ± 0.3 | 9.4 ± 0.7 | 4.9 ± 1.0 |

[29]. The dimerized β-subunit has greater thermal stability than the monomer.

It has been shown that the bis-histidyl coordination of iron in hexacoordinated hemoglobins greatly increases the rate of $Fe^{3+}$ reduction when compared to pentacoordinate hemoglobins, while the auto-oxidation rate is low [30]. In myoglobin and leghemoglobin, reduction is limited by the rate constant for electron transfer, whereas in the hexacoordinate hemoglobins reduction is limited only by bimolecular binding of the reductant [30]. The tertiary structure of barley Hb is resistant to auto-oxidation only when the cysteine is present. This may indicate its role in protection against auto-oxidation and involve tertiary structure maintenance linked to the direct participation in reduction of the heme iron.

The observed NAD(P)H-dependent scavenging activity of purified rHb and mutHb is extremely low which can be explained by slow rate of chemical reduction of metHb in the presence of NAD(P)H. To be an effective NO scavenger, metHb should be effectively reduced in a joint reaction catalyzed by a specific reductase [4]. This would explain the very high rates of NO scavenging observed in plant root extracts [3,4]. We report in a separate paper [4] on such a reductase operating with similar efficiency both with rHb and mutHb and using ascorbate as electron donor. The data presented in [4] also argue against a role of $Cys^{79}$ in an NO-scavenging mechanism.

In conclusion, $Cys^{79}$ is important for the dimeric organization of barley Hb, via disulfide bond formation, to stabilize its quaternary structure and contribute to the maintenance of the heme iron in the ferrous state. Since the cysteine participates in the formation of an intermolecular disulfide bond, its involvement in nitric oxide detoxification is unlikely. This has been demonstrated by direct measurement of nitric oxide scavenging by non-mutated and mutated barley hemoglobins in the presence of NADH and NADPH, which showed that cysteine-79 does not participate directly in the reaction of NO conversion. However to keep the Hb molecule functional and to maintain NO metabolism effectively for a prolonged time, the stability of the molecule and its resistance to auto-oxidation is crucial, and this is provided by the conserved cysteine residue.

## Acknowledgments

The skilful technical assistance of Doug Durnin is gratefully acknowledged. We thank Cyril Appleby for helpful suggestions. This work was supported by the Natural Sciences and Engineering Research Council of Canada and Genome Canada.

## References

[1] E.R. Taylor, X.Z. Nie, A.W. MacGregor, R.D. Hill, A cereal haemoglobin gene is expressed in seed and root tissues under anaerobic conditions, Plant Mol. Biol. 24 (1994) 853–862.
[2] C. Dordas, B.B. Hasinoff, A.U. Igamberdiev, N. Manac'h, J. Rivoal, R.D. Hill, Expression of a stress-induced hemoglobin affects NO levels produced by alfalfa under hypoxic stress, Plant J. 35 (2003) 763–770.
[3] A.U. Igamberdiev, C. Seregélyes, N. Manac'h, R.D. Hill, NADH-dependent metabolism of nitric oxide in alfalfa root cultures expressing barley hemoglobin, Planta 219 (2004) 95–102.
[4] A.U. Igamberdiev, N.V. Bykova, R.D. Hill, Nitric oxide scavenging by barley hemoglobin is facilitated by a monodehydroascorbate reductase-mediated ascorbate reduction of methemoglobin, Planta 223 (2006) 1033–1040.
[5] M.S. Hargrove, E.A. Brucker, B. Stec, G. Sarath, R. Arredondo-Peter, R.V. Klucas, J.S. Olson, G.N. Phillips Jr., Crystal structure of a nonsymbiotic plant hemoglobin, Structure 8 (2000) 1005–1014.
[6] B. Trevaskis, R.A. Watts, C.R. Andersson, D.J. Llewellyn, M.S. Hargrove, J.S. Olson, E.S. Dennis, W.J. Peacock, Two hemoglobin genes in *Arabidopsis thaliana*: the evolutionary origins of leghemoglobins, Proc. Natl. Acad. Sci. USA 94 (1997) 12230–12234.
[7] P.M. Strozycki, W.M. Karlowski, Y. Dessaux, A. Petit, A.B. Legocki, Lupine leghemoglobin I: expression in transgenic Lotus and tobacco tissues, Mol. Gen. Genet. 263 (2000) 173–182.
[8] T. Uchiumi, R. Kuwashiro, J. Miyamoto, M. Abe, S. Higashi, Detection of the leghemoglobin gene on two chromosomes of *Phaseolus vulgaris* by in situ PCR linked-fluorescent in situ hybridization (FISH), Plant Cell Physiol. 39 (1998) 790–794.
[9] Y. Cheng, T.J. Shen, V. Simplaceanu, C. Ho, Ligand binding properties and structural studies of recombinant and chemically modified hemoglobins altered at beta 93 cysteine, Biochemistry 41 (2002) 11901–11913.
[10] S. Hirota, K. Azuma, M. Fukuba, S. Kuroiwa, N. Funasaki, Heme reduction by intramolecular electron transfer in cysteine mutant myoglobin under carbon monoxide atmosphere, Biochemistry 44 (2005) 10322–10327.
[11] S. Dewilde, L. Kiger, T. Burmester, T. Hankeln, V. Baudin-Creuza, T. Aerts, M. Marden, R. Caubergs, L. Moens, Biochemical characterization and ligand binding properties of neuroglobin, a novel member of the globin family, J. Biol. Chem. 276 (2001) 38949–38955.
[12] D. Hamdane, L. Kiger, S. Dewilde, B.N. Green, A. Pesce, J. Uzan, T. Burmester, T. Hankeln, M. Bolognesi, L. Moens, M.C. Marden, The redox state of the cell regulates the ligand binding affinity of human neuroglobin and cytoglobin, J. Biol. Chem. 278 (2003) 51713–51721.
[13] T. Suzuki, O.H. Kapp, T. Gotoh, Novel S–S loops in the giant hemoglobin of *Tylorrhynchus heterochaetus*, J. Biol. Chem. 263 (1988) 18524–18529.
[14] K. Fushitani, M.S. Matsuura, A.F. Riggs, The amino acid sequences of chains a, b, and c that form the trimer subunit of the extracellular hemoglobin from *Lumbricus terrestris*, J. Biol. Chem. 263 (1988) 6502–6517.

[15] L.T. Tam, G.P. Gray, A.F. Riggs, The hemoglobins of the bullfrog *Rana catesbeiana*. The structure of the beta chain of component C and the role of the alpha chain in the formation of intermolecular disulfide bonds, J. Biol. Chem. 261 (1986) 8290–8294.

[16] M. Couture, M. Guertin, Purification and spectroscopic characterization of a recombinant chloroplastic hemoglobin from the green unicellular alga *Chlamydomonas eugametos*, Eur. J. Biochem. 242 (1996) 779–787.

[17] S.M.G. Duff, J.B. Wittenberg, R.D. Hill, Expression, purification, and properties of recombinant barley (*Hordeum* sp.) hemoglobin. Optical spectra and reactions with gaseous ligands, J. Biol. Chem. 272 (1997) 16746–16752.

[18] A. Shevchenko, O.N. Jensen, A.V. Podtelejnikov, F. Sagliocco, M. Wilm, O. Vorm, A. Mortensen, A. Shevchenko, H. Boucherie, M. Mann, Linking genome and proteome by mass spectrometry: large-scale identification of yeast proteins from two dimensional gels, Proc. Natl. Acad. Sci. USA 93 (1996) 14440–14445.

[19] A. Stensballe, S. Andersen, O.N. Jensen, Characterization of phosphoproteins from electrophoretic gels by nanoscale Fe(III) affinity chromatography with off-line mass spectrometry analysis, Proteomics 1 (2001) 207–222.

[20] I.V. Chernushevich, W. Ens, K.G. Standing, Orthogonal-injection TOF MS for analyzing biomolecules, Anal. Chem. 71 (1999) 452A–461A.

[21] A.V. Loboda, A.N. Krutchinsky, M. Bromirski, W. Ens, K.G. Standing, A tandem quadrupole/time-of-flight mass spectrometer with a matrix-assisted laser desorption/ionization source: design and performance, Rapid Commun. Mass Spectrom. 14 (2000) 1047–1057.

[22] M.F. Bean, S.A. Carr, Characterization of disulfide bond position in proteins and sequence analysis of cysteine-bridged peptides by tandem mass spectrometry, Anal. Biochem. 201 (1992) 216–226.

[23] M.D. Jones, S.D. Patterson, H.S. Lu, Determination of disulfide bonds in highly bridged disulfide-linked peptides by matrix-assisted laser desorption/ionization mass spectrometry with postsource decay, Anal. Chem. 70 (1998) 136–143.

[24] J. Zhou, W. Ens, N. Poppe-Schriemer, K.G. Standing, J.B. Westmore, Cleavage of interchain disulfide bonds following matrix-assisted laser desorption, Int. J. Mass Spectrom. Ion Processes 126 (1993) 115–122.

[25] K. Shirabe, T. Yubisui, T. Nishino, M. Takeshita, Role of cysteine residues in human NADH-cytochrome $b_5$ reductase studied by site-directed mutagenesis. Cys-273 and Cys-283 are located close to the NADH-binding site but are not catalytically essential, J. Biol. Chem. 266 (1991) 7531–7536.

[26] H. Sugimoto, M. Makino, H. Sawai, N. Kawada, K. Yoshizato, Y. Shiro, Structural basis of human cytoglobin for ligand binding, J. Mol. Biol. 339 (2004) 873–885.

[27] E. Vinck, S. van Doorslaer, S. Dewilde, L. Moens, Structural change of the heme pocket due to disulfide bridge formation is significantly larger for neuroglobin than for cytoglobin, J. Am. Chem. Soc. 126 (2004) 4516–4517.

[28] D. Hamdane, L. Kiger, S. Dewilde, J. Uzan, T. Burmester, T. Hankeln, L. Moens, M.C. Marden, Hyperthermal stability of neuroglobin and cytoglobin, FEBS J. 272 (2005) 1076–1084.

[29] T. Yamaguchi, J. Pang, K.S. Reddy, H.E. Witkowska, S. Surrey, K. Adachi, Expression of soluble human β-globin chains in bacteria and assembly in vitro with α-globin chains, J. Biol. Chem. 271 (1996) 26677–26683.

[30] T.R. Weiland, S. Kundu, J.T. Trent, J.A. Hoy, M.S. Hargrove, Bis-histidyl hexacoordination in hemoglobins facilitates heme reduction kinetics, J. Am. Chem. Soc. 126 (2004) 11930–11935.